PGPS: A Context-Aware Technique to Perceive Carrier Behavior from GPS Data

Chung-Hsien Tsai[1], Jiung-Yao Huang[2]
[1] Department of CSIE, Chung Cheng Institute of Technology, National Defense University, Taiwan
[2] Department of CSIE, National Taipei University, Taiwan
1keepbusytsai@gmail.com, 2jyhuang@mail.ntpu.edu.tw

Abstract

This paper presents an approach for perceiving GPS carrier behavior from GPS data only; hence, it is called perceptive GPS (PGPS). The proposed method first extracts behavior feature from GPS data to classify a carrier's current state. The Newton Hidden Markov Model (NHMM), which integrates Newton's laws of motion with a Hidden Markov Model, is then introduced to model a GPS carrier's motion state. On the basis of the NHMM, the PGPS technique records the GPS carrier's habitual behavior in a Transition Probability Matrix (TPM), which is then used to infer the behavior of the GPS carrier from the online received GPS data. This paper also presents a series of experiments that were conducted to validate the PGPS technique and to determine the proper parameters for the algorithm. By successfully perceiving GPS carrier behavior, the system can provide more friendly services such as improving the accuracy of GPS positioning, providing live view navigation, and detecting if the GPS carriers go astray during navigation.

Keywords: Augmented reality, Context-aware, Hidden Markov Model, Entropy

1 Introduction

The rapid evolution of computing technology has been accompanied by the steady development and realizability of the pervasive environment envisioned by Mark Weiser [1]. In this regard, the key issue is how to enable the environment to be aware of the existence and behavior of human beings. Such perception techniques are collectively referred to as context awareness [2]. Studies on context awareness focus on enhancing the quality of human life by perceiving the intention of a user. The use of GPS for location-based services, such as those in GPS navigation devices, is the most well-known context-aware application [3]. The design of a context-aware service on the basis of hardware sensor data involves three key issues: context extraction, behavior modeling, and behavior perception [4].

The motion of users and their habitual behavior are two important clues for inferring a user's status. However, the raw data from sensors only denote the relative signal strength between the user and the user's environment. This data requires further extraction into feature data through a so-called context extraction process [5] to become useful information for inferring a user's behavior.

A human being always has a specific behavior pattern within a period of time, and the habitual behavior can be represented by a mathematical model [6-7]. Hence, the second task of a context-aware study is to find a mathematical model that can portray a user's behavior pattern. However, human behavior patterns may change and be refined with time and variations in the environment. Hence, a good behavior model should be able to automatically adapt to the migration of the behavior pattern.

With the help of a behavior model, we can infer a user's intent from sensor data and his/her previous state. A proper service can then be pushed to the user automatically. However, the inference process should be sufficiently fast to cope with the continuously received sensor data. If the inference is too slow, the user may already switch to another state before the inference process is completed.

Based on the above three issues, this paper presents a context-aware technique using GPS data on a mobile device. From the real-time collected GPS data, the proposed technique can interactively track the driving behavior of the GPS carrier. An important application of this technique is live view navigation [8], which provides a user-centric intuitive driving navigating service. Given that no digital map is used, the motion status of the vehicle, i.e., the GPS carrier, is the crucial information for tagging a stable augmented guiding arrow on the windsheld. Using the awareness of the vehicle's current status during live view navigation, the system could also detect whether or not the driver has deviated from the scheduled route and is lost. Although several studies [9] have attempted to normalize driving behavior from the driving style, these studies utilized a

*Corresponding Author: Chung-Hsien Tsai; E-mail: keepbusytsai@gmail.com
DOI: 10.3966/160792642018091905013

quantitative method to index different driving behaviors. The driving behavior is an essential clue to determine a driving style and can be used to elucidate a driving pattern. Hence, such a GPS-based driving behavior tracking technique can be helpful for supporting traffic safety norms such as speed limit enforcement for reducing the risk of possible accidents. When combined with an automobile insurance program, this driving behavior information could be used to assess driver's insurance on the basis of driving habits and patterns [10]. The presented technique, based on the assumption that a GPS carrier is a rigid body, adopts Newton's laws of motion to design a driver's behavior model. A Hidden Markov Model is further used to capture the GPS carrier's behavior and to infer its current state. Since the approach uses GPS data only to perceive the carrier's habitual behavior, the presented technique is called Perceptive GPS (PGPS).

2 Related Work

Previous context-aware studies on modeling and reasoning a carrier's behaviors from GPS data can be classified into time-series and state-space models [11-14]. The time-series model is based on past temporal GPS raw data to profile human behaviors. For example, Patterson et al. [11] utilized joint conditional probabilities between GPS data of a user's historical footprint and the geometry of terrain to predict the user's transport behaviors and then infer the user's location. In contrast to the time-series model, which is usually limited by the past finite GPS data and the inability to infer complicated environmental information, the state-space model classifies GPS data into abstract state space in order to model the user's behavior and then infer the user's location. The advantage of the state-space model approach is that it can reason a carrier's behavior without being influenced by the fixed length of the GPS data. It can also easily couple with inertial data to dramatically reduce the computational complexity. For example, [12] applied a state-space model to GPS data collected from animals to observe animal behaviors.

Most state-space model studies are based on environment types for predicting a subject's motion state. [13] applied hierarchical Conditional Random Fields (CRFs) to sensor data collected from different vehicles to infer their respective transportation patterns. Owing to the lack of speed and acceleration information, this method is only feasible for monotonic or long-distance moving behaviors. However, the study did not consider the GPS carrier's live motion states, which means that they are not applicable to an unprepared environment.

According to the modeling method, state-space models can be broadly divided into two types: discrete and continuous [14]. Discrete state-space models use a predefined state model approach to perform prediction. A typical modeling approach for this type of model is a Kalman filter, which assumes that the modeled system is a linear noise system, to carry out state prediction and to fix sensor data errors. Although a nonlinear model for the Unscented Kalman filter method has been proposed to calibrate the sensor error, this model is too complicated and too difficult to implement on a mobile platform. Although precise motion states are expected, Interacting Multiple Model (IMM) [15] configurations with a bank of Kalman filters are often used to capture various motion states. For example, the Constant Velocity (CV) produces straight trajectories of the vehicle state. The Constant Acceleration (CA) or Coordinated Turn (CT) considers sharp turns and the accelerations of the vehicle state. These Kalman filter methods seldom have a systematic motion state modeling approach for all types of Newtonian mechanics.

All of the models discussed above are based on the assumption of a known or prepared environment. The goal of this research is to perceive a carrier's behaviors from GPS data alone without specifically observing them. To achieve this goal, a context-aware technique, as shown in Figure 1, is employed to explore the received NMEA-0183-formatted GPS data and to perceive a GPS carrier's behavior accordingly. Since the GPS data represents a snapshot of the changes in the momentum of the carrier, the characteristics of user behavior are first extracted from the received GPS data, as shown in Figure 1 and discussed in Sec. 3.2. Newton's laws of motion are then adopted to interpret the GPS data by classifying the user's current possible state. This aspect is fully explored in Sec. 3.3. An enhanced Hidden Markov Model that integrates Newton's laws of motion, called Newton Hidden Markov Model (NHMM), is designed to predict carrier behavior from GPS data that is explained in Sec. 3.4. The predicted state and classified user state are then cross-checked to determine the user's most likely current state, which is called perceived state and is explained in Sec. 3.5. Finally, since the perception of GPS carrier's behavior is based on NHMM, the information-theoretic approach used to capture such behavior is called Transition Probability Matrix (TPM). The TPM is a pre-trained user behavior matrix that we outline in Sec. 3.1 and will be amended online according to the user behavior changes, as discussed in Sec. 3.6.

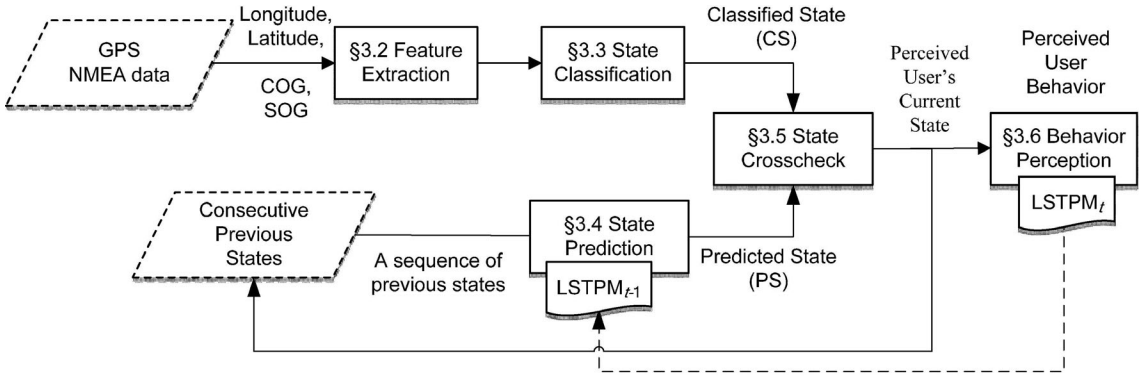

Figure 1. PGPS process flow

3 Rationale of PGPS

3.1 The Rationale

Before designing the behavior model of the GPS carrier, the assumptions of the model need to be discussed first. Since GPS data are, in essence, the position of a single point, the position information of a GPS carrier can be regarded as a snapshot of the trajectory of a rigid body. Furthermore, since the motion of the GPS carrier is much smaller than the speed of light, the mass of the carrier is unchanged during the movement. On the basis of the above two observations, we can safely assert that the movement of the GPS carrier follows Newton's laws of motion, which become the basis of this study.

By accounting the effects of Newton's laws of motion on the rigid body, the states of a GPS carrier can be categorized into seven states including the Stationary state (S_s), Linear Cruise state (S_{lc}), Veering Cruise state (S_{vc}), Linear Acceleration state (S_{la}), Veering Acceleration state (S_{va}), Linear Deceleration state (S_{ld}), and Veering Deceleration state (S_{vd}). With these predefined seven states, i.e., $\mathbf{S}$ = {S_s, S_{la}, S_{lc}, S_{ld}, S_{va}, S_{vc}, S_{vd}}, the study is specifically limited to perceive if the carrier is in one of these seven states. Further, on the basis of Newton's laws of motion, the state transition of a rigid body can be modeled as shown in Figure 2.

The color-dash line between states represents the transition possibility between two states. The black dashed line represents the state transition without any external force; the red dashed line represents the results of state transition with external positive force; the blue dashed line represents the transition react to external opposite force. However, such a transition is not directly observable from the GPS data; only a snapshot of the transition result is perceivable. Hence, the study adopts a Hidden Markov Model [16] to explore the transition probability among these seven states. The behavior model in Figure 2 is called an NHMM and becomes the perception model of PGPS.

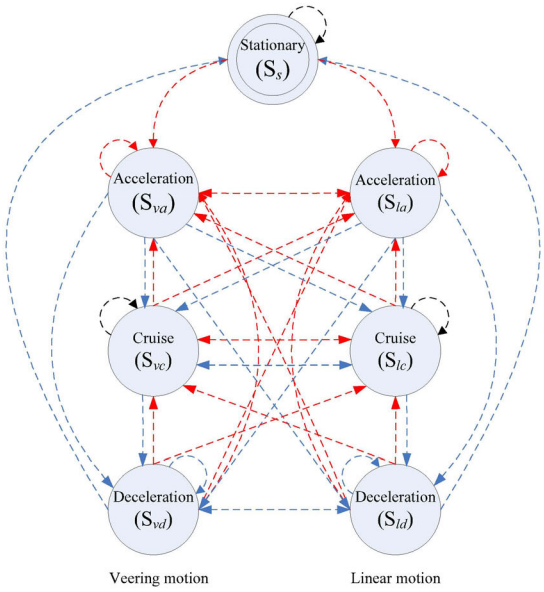

Figure 2. Newton Hidden Markov Model of PGPS

As an NHMM delimits, a GPS carrier can transit from one state to any of the seven states at the next instance of time. Thus, a 7×7 probability matrix called the TPM is designed to model the habitual behavior of the GPS carrier. The TPM is pre-trained by a sequence of logged GPS data. Let $A_{ij}(t)$ be the transition probability from state i to state j at a discrete time t; then, TPM can be formulated by Eq. (1), where $A_{ij}(t) = P(S_t = j \mid S_{t-1} = i)$, and N is the number of states.

$$\mathrm{TPM} = [P(S_t = j \mid S_{t-1} = i)]_{N\times N} = \left[A_{ij}(t)\right]_{N\times N} \quad \textbf{(1)}$$

Since a sequence of states represents the behavior of the GPS carrier in a specific period, different state sequences may train various TPMs. The study further adopts intentional motion learning and protection method [17] to identify if a TPM already reaches a stable condition in order to capture the habitual behavior of the carrier in that period of time. Hence, we define the differences between two consecutive TPMs as the entropy of the carrier's momentum. The entropy is then formulated by Eq. (2), where A_{ij}^t

indicates the transition possibility from state *i* to state *j* in the observable state sequence O_t.

$$H_t = \left| TPM_t - TPM_{t-1} \right| = \sqrt{\sum_{\forall i,j} \left(A_{ij}^{t+1} - A_{ij}^{t} \right)^2} \quad \textbf{(2)}$$

The variation in the entropy can denote the changes in the carrier's behavior. A lower entropy implies a close similarity between consecutive TPMs, which further implies the stability of the behavior of that specific period. However, we cannot immediately tell whether a system reaches its stable state at a specific moment by simply checking if its entropy, H_t, is lower than a threshold. If consecutive entropies are all within the same threshold, we can then claim that the carrier is reaching its local stable behavior. Hence, Eq. (3) is designed to detect the change in the entropy.

$$\psi(t) = \left| H_t - H_{t-1} \right| \quad \textbf{(3)}$$

Given a threshold value ε, when the entropy disparity, $\psi(t)$, approaches ε, it implies that the system is reaching a local stable behavior with the threshold value ε. At this moment, we define the average of TPM_t, TPM_{t-1}, and TPM_{t-2} as the Local Stable TPM, called $LSTPM_t$, that represents the stable local behavior of the GPS carrier. $LSTPM_t$ is then used to predict the GPS carrier's succeeding state until a new LSTPM is reached. The LSTPM is initially computed offline from a sequence of training data and is used to predict the user's current state base on the user's previous pose.

Table 1. Summary of classification rules

$\Delta\theta$ & Δx & Δv	$\lvert\Delta v\rvert < \alpha_v$	$\Delta v > \alpha_v$	$\Delta v < -\alpha_v$
$\lvert\Delta\theta\rvert \le \alpha_\theta$ & $\lvert\Delta x\rvert < \alpha_v$	Group 0 (Stationary state)	Group X (Unclassified state)	Group X (Unclassified state)
$\lvert\Delta\theta\rvert \le \alpha_\theta$ & $\lvert\Delta x_i - \Delta x_{i-1}\rvert \le \alpha_x$	Group 1 (Linear cruise state)	Group X (Unclassified state)	Group X (Unclassified state)
$\lvert\Delta\theta\rvert \le \alpha_\theta$ & $\lvert\Delta x_i - \Delta x_{i-1}\rvert > \alpha_x$	Group X (Unclassified state)	Group 2 (Linear acceleration state)	Group 3 (Linear deceleration state)
$\lvert\Delta\theta\rvert > \alpha_\theta$ & $\lvert\Delta x_i - \Delta x_{i-1}\rvert \le \alpha_x$	Group 4 (Veering cruise state)	Group X (Unclassified state)	Group X (Unclassified state)
$\lvert\Delta\theta\rvert > \alpha_\theta$ & $\lvert\Delta x_i - \Delta x_{i-1}\rvert > \alpha_x$	Group X (Unclassified state)	Group 5 (Veering acceleration state)	Group 6 (Veering deceleration state)
$\lvert\Delta\theta\rvert > \alpha_\theta$ & $\lvert\Delta x\rvert \le \alpha_x$	Group 0 (Stationary state)	Group X (Unclassified state)	Group X (Unclassified state)

3.2 Feature Extraction

When GPS data are received, the PGPS mechanism begins by trying to classify a carrier's behaviors from the received GPS data, as illustrated in Figure 1. At present, among the GPS data formats, NMEA 0183 is the most widely used standard. The NMEA 0183 format regulates the longitude, latitude, speed, UTC time, orientation, satellite information, etc. into more than ten different sentences. On the basis of Newton's laws of motion, a change in the momentum results from the exertion of an external force and causes changes in the position, velocity, and course between two consecutive GPS data points. Since the location information of the GPS data is in the form of latitude and longitude, the Haversine formula is adopted to compute the change in the position. Consequently, the displacement (Δx), velocity difference (Δv), and course difference ($\Delta\theta$) of two consecutive GPS data points are extracted as the feature data to detect the change in the behavior of the GPS carrier.

3.3 State Classification

After the feature data are extracted, as shown in Figure 1, they are then used to "guess" the current state of the GPS carrier from the GPS data directly. The speculation is conducted by classifying feature data into categories that correspond to the seven predefined states, $\mathbf{S} = \{S_s, S_{la}, S_{lc}, S_{ld}, S_{va}, S_{vc}, S_{vd}\}$, as depicted in Figure 2. The classification approach is carried out by defining the appropriate threshold values, α_x, α_v, and α_θ, for Δx, Δv, and $\Delta\theta$, respectively. However, the order of performing classification is also very important. Newton's second law of motion tells us that a change in the momentum may be caused by an alteration of the mass or a variation in the velocity. Under the assumption that the GPS carrier is a rigid body, its mass is fixed, and the change in the momentum is dominated by the variation in the velocity. Consequently, Δv should be the first key for classifying the GPS carrier's behavior from the received GPS data. Further, there is no doubt that a GPS ranging error is indeed embedded in the value of the displacement Δx, which naturally becomes the second classification key. Finally, the difference in the course, $\Delta\theta$, is the last component for classification. Hence, the feature data (Δv, Δx, $\Delta\theta$) are used to classify the received GPS data into seven groups, which then become the hidden states of the GPS carrier. Hence, according to the predefined states in Figure 2, the following rules classify the GPS carrier's states from the received GPS data into seven

groups:

- Stationary state (S_s) group: when the GPS carrier is at a standstill at a fixed position, the displacement (Δx), and the change in the velocity (Δv) should be zero. However, owing to the GPS data drift error, received GPS data with feature data, Δx and Δv, less than their respective threshold values can be recognized to be in the stationary state, S_s. To facilitate the discussion in the rest of this paper, this group is called Group 0.
- Linear Cruise state (S_{lc}) group: when the GPS carrier is moving at a constant speed in a straight line, the displacement (Δx) should maintain a constant value, and the values of the velocity (Δv) and course ($\Delta\theta$) should be zero. Owing to the GPS data drift error, consecutive values of Δx cannot be guaranteed to be constant. Hence, if Δv and $\Delta\theta$ are less than their predefined thresholds and the absolute difference between two consecutive values of Δx is less than the threshold, then the carrier is claimed to be in the Linear Cruise state, S_{lc}. This group of states is called Group 1.
- Linear Acceleration state (S_{la}) group: when the GPS carrier is acted upon by a constant force in a straight line, the displacement (Δx) and the change in the velocity (Δv) should be increased while its course ($\Delta\theta$) remains zero. To accommodate the GPS data drift error, if the absolute difference between two consecutive values of Δx and the value of Δv are greater than their thresholds while $\Delta\theta$ is less than a threshold, this situation can be defined as the GPS carrier being in the Linear Acceleration state, S_{la}. This group of states is denoted as Group 2.
- Linear Deceleration state (S_{ld}) group: when the GPS carrier is in a state with a constant reciprocal force that linearly decreases its speed, the displacement (Δx) should still be increasing while the change in the velocity (Δv) is decreasing, and the course ($\Delta\theta$) is zero. To cope with the GPS data drift error, if the absolute difference between two consecutive values of Δx and the absolute value of Δv are greater than their threshold values, if Δv is a negative value, and if $\Delta\theta$ is less than its predefined threshold, the GPS carrier is said to be in the Linear Deceleration state, S_{ld}. This group of states is called Group 3.
- Veering Cruise state (S_{vc}) group: when the GPS carrier is moving at a constant speed while changing its direction, the displacement (Δx) should be maintained at a constant value while the change in the velocity (Δv) should be zero and the absolute value of the course ($\Delta\theta$) should remain nonzero. To deal with the GPS data drift error, if the absolute difference between two consecutive values of Δx and the absolute value of Δv are less than their threshold values and $\Delta\theta$ is greater than its threshold, the GPS carrier is said to be in the Veering Cruise state, S_{vc}. This group of states is called Group 4.
- Veering Acceleration state (S_{va}) group: when the GPS carrier increases its speed and changes its direction simultaneously, both the displacement (Δx) and the change in the velocity (Δv) should increase, and the absolute value of the course ($\Delta\theta$) should be nonzero. To adapt to the GPS data drift error, if the absolute difference between two consecutive values of Δx, the value of Δv, and the absolute value of $\Delta\theta$ are greater than their thresholds, the GPS carrier is said to be in the Veering Acceleration state, S_{va}. This group of states is called Group 5 in the subsequent discussion.
- Veering Deceleration state (S_{vd}) group: when the GPS carrier is decelerating and changing its direction at the same time, the displacement (Δx) should be increasing, whereas the change in the velocity (Δv) should be decreasing, and the course ($\Delta\theta$) should be nonzero. To deal with the GPS data drift error, if the absolute difference between two consecutive values of Δx is greater than its threshold, if the absolute values of Δv and $\Delta\theta$ are greater than their thresholds, and if Δv is negative, the GPS carrier is said to be in the Veering Deceleration sate, S_{vd}. Hence, the set of GPS data recognized to be in the Veering Deceleration state is called Group 6.

Although the classification rules are derived from Newton's laws of motion, owing to the GPS data ranging error, some classified states violate the laws of nature; hence, they are collectively called Group X. In order to differentiate the above classified states from the predicted states discussed in the next section, they are collectively called the Classified State (CS) of the GPS carrier. Note that the CS is one of the seven states depicted in Figure 2, and Table 1 summarizes the classification results.

3.4 State Prediction

Owing to the existence of a GPS ranging error, a CS cannot provide a reliable current state for the GPS carrier. Hence, the habitual behavior of a human being offers a clue for detecting the possible ranging error. According to the NHMM and entropy theory, this study uses an LSTPM to record the habitual behavior of the GPS carrier. Therefore, the PGPS mechanism employs an LSTPM to predict the GPS carrier's current state, as shown in the State Prediction stage in Figure 1.

This prediction is conducted by finding the maximum transition probability to all possible current states from a known prior states. To further increase the accuracy of the prediction, this research adopts two consecutive previous states *i, j* to predict the most likely current state *k.* Hence, the LSTPM is extended to a three-dimensional state transition matrix as

$$\text{LSTPM} = [P(S_t = k \mid S_{t-2} = i \,\&\, S_{t-1} = j)]_{N\times N} = \left[A_{i,j,k}(t)\right]_{N\times N\times N} \quad \textbf{(4)}$$

As a result, Eq. (5) is used to compute the maximum probability of the current state from the two previous states and LSTPM. That is, Eq. (5) computes the state that has the maximum value among $A_{i,j,k}$ for all k with the two given consecutive previous states i and j. The state from Eq. (5) can be one of the seven states shown in Figure 2 and is generally called the Predicted State (PS) hereafter.

$$P(S_k \mid LSTPM, S_i, S_j) = \underset{given\ i,j}{\arg\max}\{A_{i,j,k} \forall k\} \quad \textbf{(5)}$$

3.5 State Crosscheck

Whenever GPS data are received, the CS is first computed from Table 1, and the PS follows from Eq. (5). As illustrated in Figure 1, these two states are then crosschecked to detect any GPS ranging error. Since the PS gives the predicted current state based on the LSTPM and the CS is the most likely current state from the received GPS data, both states are the GPS carrier's possible current states from two different sources. Hence, the inconsistency between these two states can provide the clue for detecting the existence of the GPS ranging error. Note that the PS may not be fully relied upon. For example, when $A_{i,j,k}$ is zero or the computed maximum probability is not a unique value, the result of Eq. (5) would become ambiguous. The other possible discrepancy between the PS and the CS is that both the CS and PS are correct, but the GPS carrier is currently changing its posture. Hence, when the PS is not equal to the CS, there is no absolute conclusion as to whether it means that the received GPS data have a ranging error or the prediction from Eq. (5) is incorrect. When the GPS signal has ranging errors caused by environmental effects, it implies that the CS does not follow Newton's laws of motion. Hence, PGPS will then trust the PS as the most likely current state of the GPS carrier.

A possible scenario in which the PS is incorrect may include the case where the GPS carrier is currently changing its behavior pattern or an ambiguous result is derived from Eq. (5). For example, for the first case, the GPS carrier may make a sudden change to the Linear Acceleration state (S_{la}) from the Linear Cruise state (S_{lc}). In this case, since the LSTPM records the inertial behavior of the GPS carrier, the change in the GPS carrier's inertia will also make the prediction from Eq. (5) incorrect. In order to distinguish this case from the GPS signal's ranging error, a posture threshold mechanism is designed to detect the change in the inertial status of the GPS carrier. The mechanism uses the parameter β_{pt} to record the number of consecutive state changes. If two consecutive computations of Eq. (5) are the same and both are different from the CS, the value of β_{pt} is then increased by one. An inertial threshold value φ is further defined for the GPS carrier. When $\beta_{pt} > \varphi$, the system will then believe that the inertial behavior of the GPS carrier has changed and then trust the CS as the most likely current state. On the other hand, if $\beta_{pt} \le \varphi$, we assume a GPS ranging error exists and trust the PS.

3.6 Behavior Perception

Most people will have the same habitual reaction to a similar scenario; thus, the LSTPM records the habitual behavior of a GPS carrier at that specific time frame. However, the habitual behavior of the GPS carrier may change along with the variation in its environment. At that instance, the LSTPM has to be updated, which is indicated by the dashed line from the Behavior Perception stage to the State Prediction stage in Figure 1, for follow-up inferences. Therefore, the key issue is when to replace the current LSTPM with a new one to respond to a change in the habitual behavior. According to the temporal locality of a motion pattern [18], the duration of a behavior is the major index for perceiving a change in a habitual behavior. Since this research is based on entropy theory to recognize the stability of a GPS carrier's behavior, the entropy becomes the key factor for distinguishing different habitual behaviors. Given ϕ as the tolerance value of the entropy, Eq. (3) is then further extended to Eq. (6) to detect if a local habitual behavior of a GPS carrier has changed, and the LSTPM should be updated for the follow-up inference.

$$| H_{current} - H_t | \ge \phi \quad \textbf{(6)}$$

In Eq. (6), $H_{current}$ is the entropy when the current LSTPM is computed, and H_t is the newly computed entropy from Eq. (2). In other words, different habitual behaviors will produce diverse LSTPMs, and the current LSTPM will be replaced if Eq. (6) is true.

4 Experiments

PGPS is a novel approach for perceiving a GPS carrier's behavior from GPS data only. Other than the NHMM and entropy theory, the efficiency of PGPS depends upon the proper setting of various threshold values. Hence, a series of experiments were conducted to validate the correctness of PGPS and the setting of the threshold values.

4.1 Thresholds for Classification

The study focuses on applying GPS signal data in order to perform a context-aware perception. Therefore, the availability of a GPS signal must be confirmed prior to beginning the perception process. Based on the characteristics of the GPS receiver, reliable GPS data require accurate initialization of their parameters. Because GPS positioning is based on the principle of triangulation, a GPS receiver must receive signals from at least four satellites before its data becomes usable.

Thus, the PGPS mechanism must ensure that the aforementioned criteria are satisfied before the inference process is inititaed

After initialization, the PGPS algorithm can then begin to classify the received GPS data in accordance with Table 1 to obtain a CS. The classification process is based on three threshold values (α_x, α_v, α_θ). Because the classification result will significantly affect the subsequent state inferences, selection of the proper threshold values is the primary experiment of this study.

Under reliable and stable GPS signal reception conditions, the state classification stage uses three threshold values (α_x, α_v, α_θ) to realize Table 1 with the online received GPS data. Because α_x represents a position shift between consecutive received GPS data points, the study utilizes this displacement to determine whether or not the carrier is stationary. According to Newton's first law of motion, the value of α_x is determined by the external force exerted on the GPS carrier. Since the experiment is carried out on a vehicle, we define α_x as the shortest moving distance of a vehicle when an external force is applied to complete a full spin of its tires, i.e., the circumference of a tire. According to tire specifications, the circumference of an 18-inch tire is around 2 m. Hence, α_x is set to 2 m.

Furthermore, among the received NMEA0183 format strings, the GPRMC statement contains the Speed Over Ground (SOG) value of the vehicle. Therefore, the difference between two consecutive SOG values could be considered to determine whether a GPS carrier is accelerated by any external force. In order to increase the discrimination of the driving parameter α_v, the study follows the statistical analysis method proposed in [19] to perform a normally distributed computation on 10,000 sets of SOG differences and to obtain the standard deviation of the distribution as 0.318. This value is then set as the value of α_v. The final α_θ value indicates whether or not the GPS carrier changes its forward direction and could be derived from the Course Over Ground (COG) value in the GPRMC statement of the GPS data. Since a human is driving a car, the driver's field of view is often narrowed to about 30°. Thus, the study uses 15° as the threshold value for determining whether or not the GPS carrier is changing direction.

4.2 State Perception

The PGPS algorithm infers the carrier's current state by crosschecking the PS and CS. Hence, the next issue is to confirm whether the algorithm can correctly determine the current state of the GPS carrier. An experiment was conducted wherein a vehicle is first driven on a street and then enters the highway, as shown in Figure 3(a). Then, the vehicle returns to the street from the highway, as shown in Figure 3(b). The different colored dots in Figure 3(a) and Figure 3(b) indicate the carrier's speed at each spot, and the circles mark the segments during which the carrier's speed has significant changes. These segments are all curved roads. The colored dots reveal that the driver performs a series of decelerating, turning, and accelerating behaviors in these segments, and these behaviors are what the algorithm intends to perceive. The state perception results are shown in Figure 4(a) and Figure 4(b), which correspond to Figure 3(a) and Figure 3(b), respectively. The horizontal axis of Figure 4 indicates the feature data obtained from consecutive GPS data points. The vertical axis indicates the perceived state from the State Crosscheck stage (Figure 1), the Stationary state (S_s), Linear Deceleration state (S_{ld}), Linear Cruise state (S_{lc}), Linear Acceleration state (S_{la}), Veering Deceleration state (S_{vd}), Veering Cruise state (S_{vc}), and Veering Acceleration state (S_{va}), respectively. From the experiment, it can be confirmed that PGPS accurately identifies the GPS carrier's state variation.

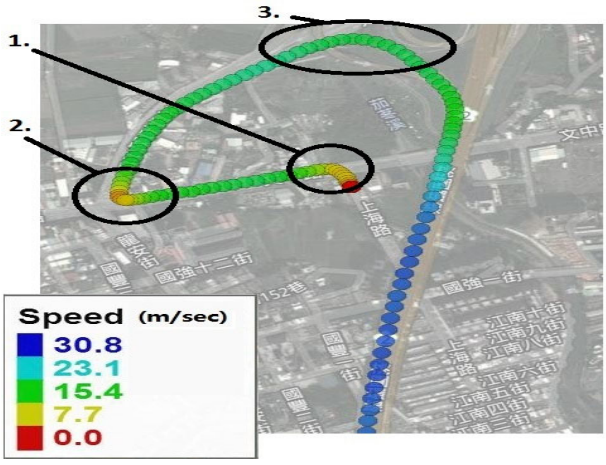

(a) Trail from the city road to the highway

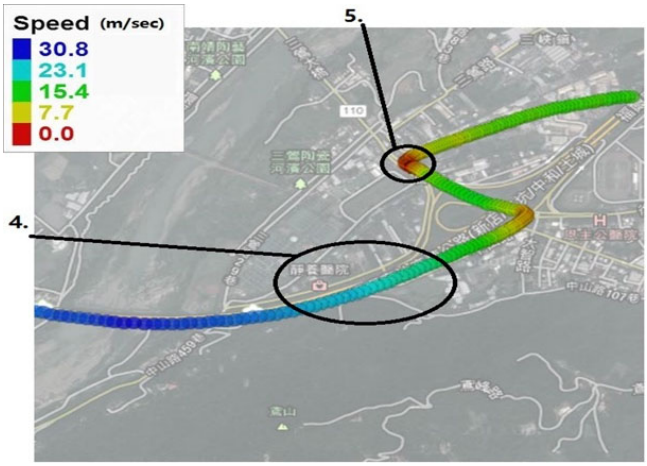

(b) Trail from the highway to the city road

Figure 3.

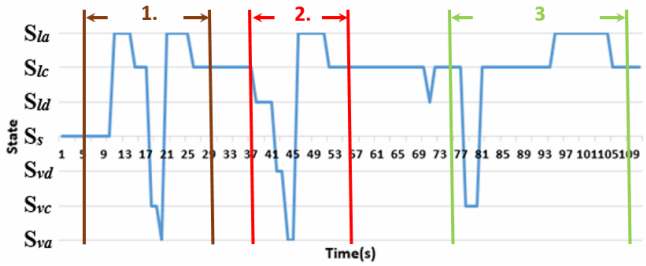

(a) State transition chart of Figure 3(a)

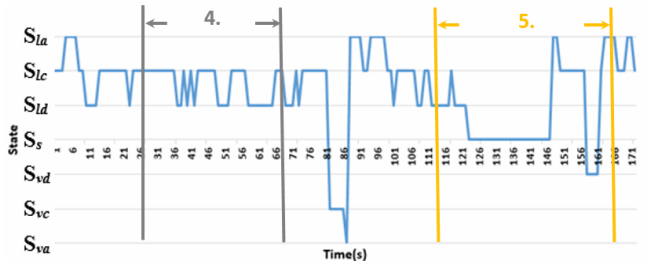

(b) State transition chart of Figure 3(b)

Figure 4.

4.3 Posture Threshold Mechanism

In addition to predicting user behavior from classified GPS data, the PGPS algorithm utilizes the carrier's previous habitual behaviors to perceive its current state. Hence, the efficiency of the PGPS mechanism to project the carrier's state from classified state and previous consecutive states requires validation. As depicted in Figure 1, the carrier's current state is inferred from a crosscheck between the PS and CS. A discrepancy between these two states occurs in two situations: either the carrier changes his/her state in response to variations in the environment, or a misjudgment occurs as a result of the effect of GPS ranging errors. To distinguish these two situations, this study designs a posture threshold to detect a change in the carrier's posture. Correct detection of the carrier's posture affects the accuracy of perception. Thus, a third experiment is conducted to determine an appropriate posture threshold value.

The state crosscheck stage (Figure 1) of PGPS further designs the posture threshold mechanism to detect if the GPS carrier is changing its inertial behavior. When the CS is different from the PS, the mechanism uses the duration of the GPS carrier that maintains the same CS value to detect if the GPS carrier is changing its current inertial behavior. Hence, the proper setting of the inertial threshold value φ determines the effectiveness of the mechanism. Because the GPS receiver receives data statements at one second intervals, the study takes one second as the posture threshold value unit.

The setting of the inertial threshold value is related to Newton's laws of motion. When the threshold value is 1, the state crosscheck stage does not consider the inertial behavior of the GPS carrier. On the basis of Newton's first law of motion, objects remain in their previous states when no external forces are present. In other words, while objects remain in the Stationary state (S_s) or Linear Cruise state (S_{lc}), they will not change without any external forces. On the other hand, the other five states in Figure 2 are assumed to occur when an external dynamic force is exerted. Hence, the inertial behaviors of S_s and S_{lc} are more significant than other five states. Therefore, their posture threshold values should be greater than the others. Furthermore, after conducting a series of experiments, it was observed that the GPS ranging error would interfere with the persistence of the CS value when the GPS carrier is changing its state. Hence, for practical operation, when the number of consecutive differences between the PS and the CS is greater than the inertial threshold value, we will assume that the GPS carrier changes its behavior without considering if the CS maintains the same value during that period.

Figure 5 shows a line chart of the states for the segment of the path in Figure 3(a) where the GPS carrier enters the highway from the interchange. In Figure 5(a), all states' inertial threshold values are set as 1, meaning that we completely trust the CS directly from the GPS data. For comparison, the inertial threshold values of the Stationary state (S_s) and Linear Cruise state (S_{lc}) are set as 2, and the other states posture threshold values are set as 1 in Figure 5(b). In Figure 5(a), the vehicle is switching into the Veering Cruise state (S_{vc}) from the Linear Cruise state (S_{lc}) between time sequences 2-6. This indicates that the GPS carrier is changing its behavior. However, the CS values jump between values of 1 and -3 owing to GPS ranging errors. In addition, because of the GPS ranging errors, state spikes are present between time sequences 40-66 in Figure 5(a) while GPS carrier moves in a steady behavior. However, these spikes are eliminated in Figure 5(b). Hence, the inertial threshold setting in Figure 5(b) is adopted.

4.4 Transition Matrix Stabilization

Finally, this study records the carrier's behaviors in a TPM based on Eq. (1) and further detects whether a carrier's behavior has reached a local stable habitual behavior by using Eq. (2) and (3). Consequently, a fourth experiment is conducted to verify whether Eq. (2) and (3) can detect a carrier's local stable habitual behavior and determine the appropriate threshold value ε.

The study utilizes Eq. (2) and Eq. (3) to detect if the GPS carriers' habitual behaviors have reached their local stability. Two issues are raised accordingly. The first issue is related to whether or not Eq. (2) and Eq. (3) can faithfully capture GPS carrier's habitual behavior changes. The second is how to find the threshold value ε for Eq. (3). Two experiments were

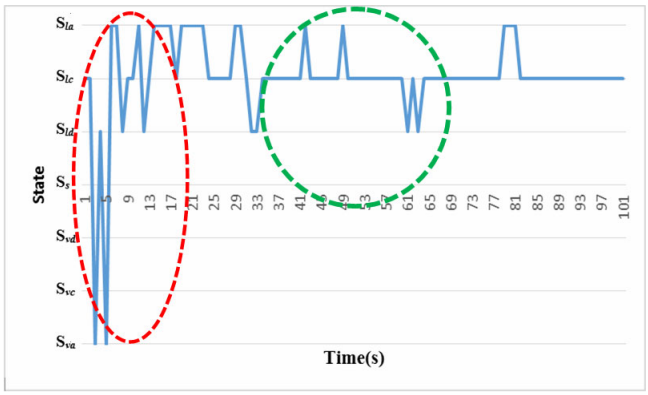

(a) State transition chart when the inertial threshold values for all states are set to 1

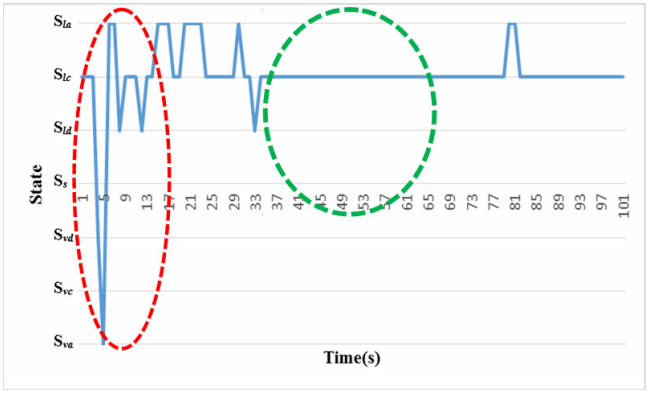

(b) State transition chart when the inertial threshold values of S_s and S_{lc} are set to 2 and all other states are set to 1

Figure 5. State histogram of Figure 3(a)

then conducted to resolve these issues. In these experiments, we grouped 150 records of consecutive GPS data sets as an observation segment. In other words, we use 150 consecutive states to build a TPM by Eq. (1). A series of entropy values is then calculated by Eq. (2). Finally, a sequence of entropy disparity values, ψ (t), which can detect the local stability of the carrier's behavior, is then derived from Eq. (3).

The track of the first experiment is shown in Figure 6, where the labels A, B, …, G denote the segments of the GPS data using 150 records as a unit. Figure 7 shows a line chart of the entropy values from Eq. (2). For example, the entropy value for segments A and B in Figure 6 is plotted at time segment 1. Figure 8 shows a line chart of the entropy disparity values from Eq. (3) for Figure 6. In other words, for example, the entropy disparity value derived from segments A, B, and C in Figure 6 is plotted at time segment 1. A comparison of the line chart in Figure 8 and the colored dots in Figure 6 shows that a low entropy disparity value will be calculated from Eq. (3) when the behaviors of the GPS carrier within three consecutive segments are similar. The experiments demonstrate that Eq. (2) and Eq. (3) could obtain the changes in the GPS carrier's habitual behavior directly from the GPS data.

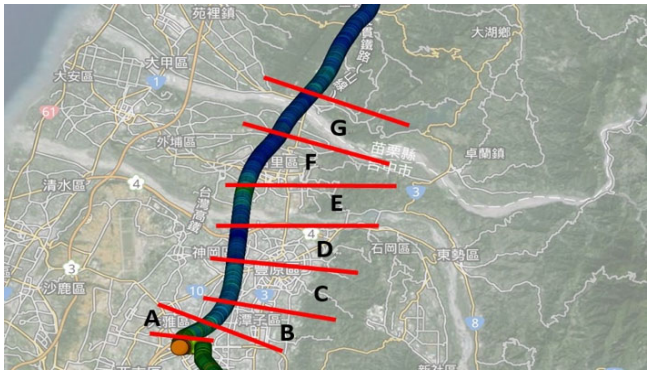

Figure 6. Track on the highway

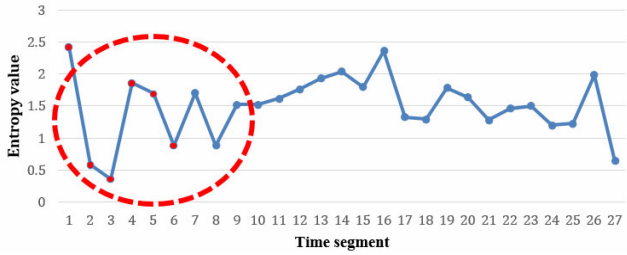

Figure 7. Line chart of the entropy values for Figure 6

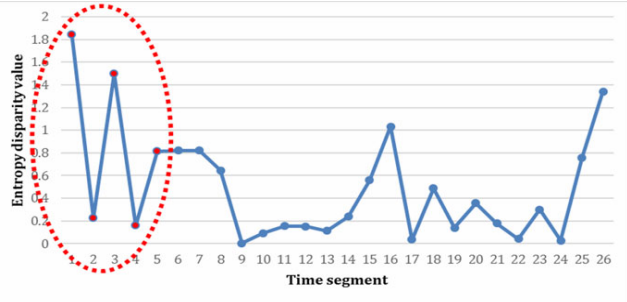

Figure 8. Line chart of the entropy disparity values for Figure 7

To determine the threshold value of Eq. (3), the study was extended to other experimental paths to collect more GPS data for further analysis, as shown as Figure 9. There are over 6,000 records of GPS data, and the calculated entropy disparity values are displayed in Figure 10. More than 50% of these entropy disparity values are between 0.1-0.5; thus, the threshold values would lie between 0.1-0.5. If the threshold value is too small, it indicates that the GPS carrier's behavior should remain consistent for a long period, which is not the case for the behavioral activities of human beings. On the contrary, if the threshold value is too high, it could not reveal the local stability of a GPS carrier's behavior. After repeating the experiments several times, the study eventually determined a threshold value of 0.4. A summary of the threshold values from the experiments is listed in Table 2.

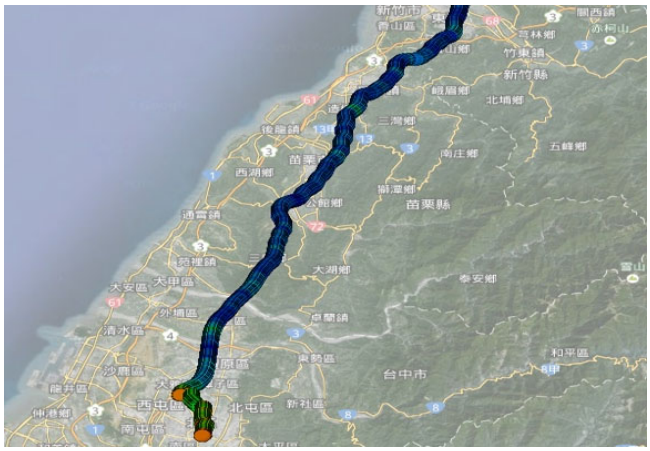

Figure 9. Track of the experiment for analyzing proper threshold value

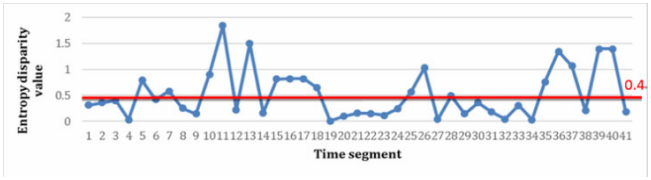

Figure 10. Chart of the entropy disparity values for Figure 10

Table 2. Summary of threshold values

Threshold	Value	number of the equation
α_x	2	tire specifications
α_v	0.318	statistical analysis method
α_θ	15°	driver's field of view
Inertial threshold	1 and 2	Newton's laws of motion
Entropy disparity	0.4	Eq. (2) and (3)

5 Conclusion

This paper presented an approach to interactively infer the behavior of a GPS carrier by utilizing a sequence of received GPS data only. Hence, the proposed approach is called PGPS. Although GPS signals are vulnerable to environmental effects, a behavior pattern still exists in the context of the received GPS data. PGPS is a novel approach that adopts GPS data as the feature evidence of a carrier's behavior. A behavior perception model that combines Newton's laws of motion and a Hidden Markov Model, called the NHMM, was presented in this paper. Furthermore, the TPM for the NHMM is a mechanism for recording the habitual behavior of the GPS carrier. Owing to the fact that human behavior may change in response to the environment, the entropy is introduced to compute the local stable behavior of the GPS carrier. A posture threshold is further designed to detect a change in the habitual behavior of the GPS carrier. Hence, with the predefined perception states of the GPS carrier, our experiments show that PGPS can successfully perceive a carrier's status through the NHMM.

The PGPS algorithm could further assist a Mobile Augmented Reality (MAR) browser to obtain a user's current browsing intent. On the basis of the inferred intent, the MAR browser could dynamically adjust the size of the tagged contents on a screen and provide the appropriate visual effects to satisfy the user's requirements [20]. Since PGPS is based on the assumption of the trajectory of a rigid body, PGPS can easily be extended to other sensors that also detect a single point of location. As a result, two research directions are currently under investigation. One is to explore PGPS for a user having a different momentum, such as pedestrian. The other is to extend the NHMM to other sensors to perceive human behavior and localisation [21].

Acknowledgments

This work was sponsored by the Ministry of Science and Technology (MOST) of Taiwan under grants MOST 105-2623-E-305-004-D

References

[1] M. Weiser, The Computer for the 21st Century, *Scientific American*, Vol. 265, No. 3, pp. 94-104, September, 1991.

[2] C. Bettini, O. Brdiczka, K. Henricksen, J. Indulska, D. Nicklas, A. Ranganathan, D. Riboni, A Survey of Context Modelling and Reasoning Techniques, *Pervasive and Mobile Computing*, Vol. 6, No. 2, pp. 161-180, April, 2010.

[3] J. Chon, H. Cha, LifeMap: A Smartphone-Based Context Provider for Location-Based Services, *IEEE Pervasive Computing*, Vol. 10, No. 2, pp. 58-67, April-June, 2011.

[4] R. DeVaul, M. Sung, J. Gips, A. Pentland, MIThril 2003: Applications and Architecture, *Seventh IEEE International Symposium on Wearable Computers*, White Plains, NY, 2003, pp. 4-11.

[5] Y. Lee, S. S. Iyengar, C. Min, Y. Ju, S. Kang, T. Park, J. Lee, Y. Rhee, J. Song, MobiCon: A Mobile Context-Monitoring Platform, *Communications of the ACM*, Vol. 55, No. 3, pp. 54-65, March, 2012.

[6] J. P. Gupta, P. Dixit, V. Bhaskar-Semwal, Analysis of Gait Pattern to Recognize the Human Activities, *International Journal of Interactive Multimedia and Artificial Intelligence*, Vol. 2, No. 7, pp. 7-16, September, 2014.

[7] V. B. Semwal, K. Mondal, G. C. Nandi, Robust and Accurate Feature Selection for Humanoid Push Recovery and Classification: Deep Learning Approach, *Neural Computing and Applications*, Vol. 28, No. 3, pp. 565-574, March, 2017.

[8] J. Y. Huang, C. H. Tsai, S. T. Huang, The Next Generation of GPS Navigation Systems, *Communications of the ACM*, Vol. 55, No. 3, pp. 84-93, March, 2012.

[9] B. Shi, L. Xu, J. Hu, Y. Tang, H. Jiang, W. Meng, H. Liu, Evaluating Driving Styles by Normalizing Driving Behavior Based on Personalized Driver Modeling, *IEEE Transactions*

on Systems, Man, and Cybernetics: Systems, Vol. 45, No. 12, pp. 1502-1508, December, 2015.

[10] A. B. Ellison, S. P. Greaves, M. C. J. Bliemer, Driver Behaviour Profiles for Road Safety Analysis, *Accident Analysis & Prevention*, Vol. 76, pp. 118-132, March, 2015.

[11] D. J. Patterson, L. Liao, D. Fox, H. Kautz, Inferring High-level Behavior from Low-level Sensors, *UbiComp 2003: Ubiquitous Computing,* Seattle, WA, 2003, pp. 73-89.

[12] T. A. Patterson, L. Thomas, C. Wilcox, O. Ovaskainen, J. Matthiopoulos, State-Space Models of Individual Animal Movement, *Trends in Ecololgy and Evolution*, Vol. 23, No. 2, pp. 87-94, February, 2008.

[13] L. Liao, D. Fox, H. Kautz, Extracting Places and Activities from GPS Traces Using Hierarchical Conditional Random Fields, *International Journal of Robotics Research*, Vol. 26, No. 1, pp. 119-134, January, 2007.

[14] J. L. Crowley, J. Coutaz, G. Rey, P. Reignier, Perceptual Components for Context Aware Computing, *UbiComp 2002: Ubiquitous Computing*, Göteborg, Sweden, 2002, pp. 117-134.

[15] L. Hong, Multirate Interacting Multiple Model Filtering for Target Tracking Using Multirate Models, *IEEE Transactions on Automatic Control*, Vol. 44, No. 7, pp. 1326-1340, July, 1999.

[16] L. R. Rabiner, A Tutorial on Hidden Markov Models and Selected Applications in Speech Recognition, *Proceedings of the IEEE*, Vol. 77, No. 2, pp. 257-286, February, 1989.

[17] D. Vasquez, T. Fraichard, O. Aycard, C. Laugier, Intentional Motion On-line Learning and Prediction, *Machine Vision and Applications*, Vol. 19, No. 5-6, pp. 411-425, October, 2008.

[18] M. Lin, W.-J. Hsu, Mining GPS Data for Mobility Patterns: A Survey, *Pervasive and Mobile Computing*, Vol. 12, pp. 1-16, June, 2014.

[19] Z. Constantinescu, C. Marinoiu, M. Vladoiu, Driving Style Analysis Using Data Mining Techniques, *International Journal of Computers Communications & Control*, Vol. 5, No. 5, pp. 654-663, 2010.

[20] T. Höllerer, S. Feiner, D. Hallaway, B. Bell, M. Lanzagorta, D. Brown, S. Julier, Y. Baillot, L. Rosenblum, User Interface Management Techniques for Collaborative Mobile Augmented Reality, *Computers and Graphics*, Vol. 25, No. 5, pp. 799-810, October, 2001.

[21] A. Lin, J. Zhang, X. Jiang, J. Zhang, A Reliable and Energy-efficient Outdoor Localisation Method for Smartphones, *International Journal of Ad Hoc and Ubiquitous Computing*, Vol. 23, No. 3/4, pp. 230-242, January, 2016.

Biographies

Chung-Hsien Tsai is an assistant professor of Computer Science and Information Engineering at Chung Cheng Institute of Technology, National Defense University, Taiwan. He got Ph.D. degree at National Central University in 2011. His current research interests include computer vision, immersive virtual reality, mobile computing, and mobile augmented reality.

Jiung-yao Huang is a Professor in Department of Computer Science and Information Engineering at National Taipei University. He received his Ph.D. degree in Electrical and Computer Engineering from the University of Massachusetts at Amherst in 1993. His research interests include pervasive computing, augmented reality, computer graphics, and networked virtual reality.